JMEPEG (2002) 11:614-621

Influence of the Post-Deformation Annealing Heat Treatment on the Low-Cycle Fatigue of NiTi Shape Memory Alloys

Vladimir Brailovski, Patrick Terriault, and Sergei Prokoshkin

(Submitted 3 December 2001)

Shape memory alloys (SMA) suffer from the same impairing mechanisms experienced during cycling loading by classic alloys. Moreover, SMA fatigue behavior is greatly influenced by thermomechanical cycling through the zone of thermoelastic phase transformation, which is the basis of shape memory and superelasticity effects. Since the fatigue resistance of any material can be improved by an appropriate thermomechanical treatment, in the present work combined differential scanning calorimetry and micro-hardness testing were used to determine an optimum annealing temperature for the cold-worked Ni-50.1%Ti alloy. The optimization is based on the assumption that latent heat of transformation is proportional to the mechanical work generated by SMA upon heating, while material hardness is related to the yield stress of the material. It is supposed that an optimum trade-off in these two properties guarantees the best dimensional and functional stability of SMA devices. The level and stability of the mechanical work generated by the material during low-cycle fatigue testing are considered criteria for the material performance and thus of the validity of the proposed optimization procedure.

Keywords annealing, fatigue strength, shape memory alloys, thermomechanical treatment

1. Introduction

Shape memory alloys (SMAs) are sensitive to fatigue; they suffer from the same impairing mechanisms experienced by classic alloys, accompanied by other mechanisms related to their martensitic origin. Since SMAs are exclusively used for their superelasticity or memory effects, it is natural to limit fatigue studies to the cases involving a complete or partial phase transformation cycle. In this concern, a fatigue life definition for SMAs should include not only dimensional stability but also stability of their functional characteristics during mechanical, thermal, and thermomechanical cycles (Table 1). Since the fatigue resistance of SMAs can be improved by an appropriate thermomechanical treatment,[1] the present work is focused on the adequate selection of the annealing treatment for a cold-worked Ni-50.1%Ti alloy. This annealing heat treatment is generally intended to regulate shape memory properties of the cold-worked material and to set a shape into the material.

To optimize post-deformation annealing heat treatment of NiTi alloys, it is proposed in this article that two commonly used experimental techniques be combined: differential scanning calorimetry (DSC) and Vickers microhardness testing. DSC analysis has already become the most common technique for SMA characterization and quality control.[2] Hardness testing is also frequently used to control strengthening of SMAs on different steps of their thermomechanical history.[3] The idea of optimization is based on the assumption that latent heat of transformation is proportional to the mechanical work, which could be generated by SMAs upon heating, while material hardness is related to the true yield stress of the material. It is supposed that an optimum trade-off in these two properties will guarantee the best dimensional and functional stability of SMA devices.

Therefore in the present work, DSC and Vickers micro-hardness testing (HV) were used in a systematic way to determine an optimum annealing treatment for cold worked Ni-50.1%Ti alloy. Moreover, to assess the influence of the transformation induced hardening on the optimum for the annealing treatment, two differently processed sets of samples were used for combined DSC-HV testing: (a) annealed and then stress-free thermally cycled samples or (b) only annealed samples.

In the second part of the article, the results obtained by the combined use of DSC and micro-hardness techniques were validated under low-cycle fatigue testing, which consists in thermal cycling of thin ribbon specimens under uniaxial constant load. The level and stability of the mechanical work generated by the material during fatigue testing under different applied stresses are considered as criteria of the material performance, and thus of the validity of the proposed optimization procedure.

Vladimir Brailovski and **Patrick Terriault,** Department of Mechanical Engineering, Ecole de Technologie Supérieure, Université du Québec, 1100, Rue Notre-Dame Ouest, Montreal (Quebec), Canada, H3C 1K3; and **Sergei Prokoshkin,** Moscow Steel and Alloys Institute, Leninsky Prospect 4, Moscow 119991, Russia. Contact e-mail: vbrailovski@mec.etsmtl.ca.

2. Preliminary Remarks

2.1 Thermomechanical Treatment of NiTi Alloys

SMA manufacturing is a multistage process combining melting, hot forging, and rolling, followed by warm and cold

Table 1 SMA Fatigue Classification (Adapted From Van Humbeeck and Hornbogen)[8,9]

Types of SMA Fatigue	Dimensional Stability Parameters	Functional Stability Parameters
Mechanical fatigue: superelasticity (T = const.)	Residual strain	Reversible strain Martensite induction and austenite recovery stresses
Thermal fatigue: assisted two-way memory (σ = const.)	Permanent strain	Recovery strain
Thermomechanical fatigue: one- and two-way memory (T and σ = var.)	Residual strain	Recovery stress Recovery strain Critical stress for martensite Reorientation
All types of fatigue	Fracture	Characteristic temperatures Thermal and mechanical hysteresis Fatigue life

drawing or rolling alternated with heat treatment procedures. Each technological step in the material history is important with respect to its final characteristics, but the main influence on the functional properties of the given alloy is caused by final technological operations, which, as a rule, include warm or cold working as well as annealing and/or aging thermal treatments.

Two main structural features are responsible for improving fatigue resistance of NiTi alloys: (a) high density of dislocations introduced during preceding cold work (dislocation hardening), and (b) presence of fine precipitates in the alloy (precipitation hardening). For Ni-rich specimens, the improvement of the fatigue resistance can be achieved by cold working and material aging, while for Ni-poor (equiatomic) alloys the effect can be achieved by cold-working and post-deformation annealing.[1] It should be noted, however, that when a specific material is purchased and not proprietarily manufactured (the most common case), the exact technological procedures, including regimes of warm or cold working and heat treatments, are not normally known, since the information is known only by the supplier. Therefore, post-deformation heat treatment remains the most simple and effective method for eliminating excessive strain hardening, while keeping a favorable material substructure obtained during preceding plastic deformation of the material.

To make the most use of the annealing or aging heat treatments by ensuring dimensional and functional stability of SMA devices, it is necessary to determine the optimum conditions of their application in each particular case. On one hand, the higher the annealing temperature (and time, for Ni-rich alloys), the more complete is the mobility of interphase and twin boundaries and thus the shape memory effect. On the other hand, for each material having specific thermomechanical history, the lowest heat treatment temperature is normally recommended to retain the strengthening effect of cold working. Therefore, the choice of the heat-treatment conditions determines the trade-off in these two properties.

Taking into account these opposite trends, and to improve mechanical and shape memory properties of the material, Lin and Wu have proposed limiting the temperature of the post-deformation heat treatment by the finish temperature of the reverse martensitic transformation (RMT) that occurs during the first heating of severely cold-worked martensite.[4] This temperature is approximately 250-300 °C, much higher than the normal RMT temperature (up to 100-120 °C), and at the same time substantially lower than the normal annealing temperature (400-600 °C). (This phenomenon is known as high-temperature SME.) Despite successful use of this method, its applicability should be verified for each particular case because an excessive increase of critical stresses of martensite reorientation caused by severe cold working could provoke true plastic deformation of the sample during the first loading cycles.

2.2 Hardness Measurements and SMA

It should be noted that hardness of shape memory alloys—in concert with other measurable changes concomitant with thermoelastic martensitic transformation—might be of special interest in the temperature region between M_f and M_d.[5] Hardness measured at these temperatures represents a composite result of true plastic deformation of austenite and stress-induced phase transformation of austenite. A reduction of the test temperature under A_f leads to an increase of the phase transformation contribution to the indentation due to diminished stability of the austenite phase. This behavior is observed in cooling down to the M_s temperature where small stresses convert unstable austenite to martensite. In this case, the indentation could be due to the stress-induced phase transformation exclusively, and therefore it will disappear upon heating of the specimen above the A_f temperature. Finally, at temperatures under M_f, indentation mechanism is directly linked to the martensite reorientation and plastic deformation. (The latter occurs in the case of sufficiently high-applied stresses.)

Therefore, the evolution of the material hardness measured in function of temperature in the ($M_f - M_d$) range can be used to assess transformation temperatures of the alloy and not for evaluation of the material strengthening. On the contrary, the apparent material hardness measured beyond the ($M_f - M_d$) range reflects fairly relative strengthening of SMA without being concerned with martensitic transformation artifacts. In the present paper, hardness measurement will be used exclusively to characterize the strengthening of the material in the martensitic state ($T < M_f$).

3. Optimization Procedure

3.1 Formal Approach

The following two-step approach for the express selection of the best annealing temperature for NiTi alloys is proposed. The first step consists of measuring latent heat and hardness values of as-cold-worked NiTi samples subjected to isochronal post-deformation annealing treatments at temperatures varying in quite a wide region (400-700 °C, for example). Then the predictive mathematical optimization of the post-deformation annealing temperature is performed using the simple additive weighting method (SAW), probably the best known and widely used method for solving multiple criteria decision making (MCDM) problems.[6]

Mathematically, this method is stated as follows: suppose a problem having j attributes in the presence of a conflicting optimization criteria. The decision maker has to select the best alternative (set of attributes) that will be the most attractive overall conflicting criteria, by assigning a set of importance weights to different attributes, $w = \{w_1, w_2, \ldots, w_n\}$. Then the most preferred alternative, A^*, is selected such that

$$A^* = \left\{ A_i \middle| \max_i \sum_{j=1}^{n} w_j r_{ij} \Big/ \sum_{j=1}^{n} w_j \right\} \quad \text{(Eq 1)}$$

where r_{ij} is the normalized outcome of the i^{th} alternative about the j^{th} attribute with a numerically comparable scale. In the case when criteria are defined as benefits (the larger the output, the greater preference), the normalized outcome can be obtained using linear scale transformation procedure:

$$r_{ij} = \frac{x_{ij} - x_i^{min}}{x_j^* - x_j^{min}} \quad \text{(Eq 2)}$$

where $x_j^* = \max_i x_{ij}$.

The advantage of this scale transformation is that the scale of measurement varies precisely from 0 to 1 for each criterion. The worst outcome of each criterion implies $r_{ij} = 0$, while the best outcome is $r_{ij} = 1$. A possible drawback of this procedure is that this scale transformation leads to a disproportional change in the outcomes. To keep the relative order of magnitude of the outcomes equal; the outcome of each benefit criterion x_{ij} could be simply divided by its maximum value:

$$r_{ij} = x_{ij}/x_j^* \quad \text{(Eq 3)}$$

In our case, two attributes, which depend on the temperature of annealing, are considered in the model: hardness and latent heat. On one hand, the higher the latent heat of transformation, the higher the work output that can be generated by the material upon heating. On the other hand, the higher the hardness, the higher the critical stress for slip, and therefore the higher the fatigue performances of the material that can be achieved. Effectively, maximization of the latent heat and maximization of the hardness outputs represent a classic example of two conflicting objectives because a higher latent heat can be obtained only at the expense of a lower strength of the cold-worked material and vice versa. Considering that $\sum_{j=1}^{n} w_j = 1$, the preferred post-deformation heat treatment temperature, T_{opt}, can be determined from the following formula derived from Eq 1 and 2:

$$T_{opt} = \left\{ \max\left(w(\text{HV}) \cdot \frac{\text{HV}_i - \text{HV}_{min}}{\text{HV}_{max} - \text{HV}_{min}} + w(\text{LH}) \cdot \frac{\text{LH}_i - \text{LH}_{min}}{\text{LH}_{max} - \text{LH}_{min}} \right) \right\} \quad \text{(Eq 4)}$$

where $\text{HV}_i(\text{LH}_i)$, $\text{HV}_{max}(\text{LH}_{max})$, and $\text{HV}_{min}(\text{LH}_{min})$ represent current, maximum, and minimum hardness (latent heat) values measured in the region of interest; while w(HV) and w(LH) represent their importance weights.

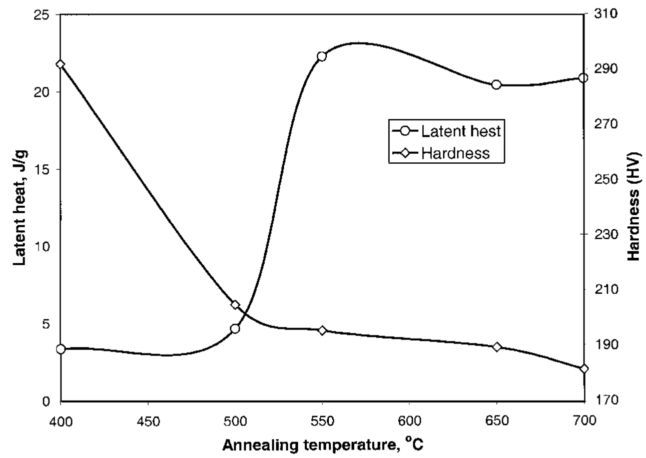

Fig. 1 Latent heat of transformation and hardness of the martensite in the function of annealing temperature (heating 1 h and cooling at ambient temperature)

4. Experimental Results

Nearly equiatomic NiTi (50.1 at.% Ti: 49.9 at.% Ni) cold-rolled ribbon was supplied by Special Metals Co. (New Hartford, NY) (approximately 25% of final cold work). The width of the ribbon is of 0.5 cm and the thickness is 0.025 cm. Figure 1 shows the results of Vickers microhardness and DSC testing of precut samples annealed during 1 h at temperatures varying between 400 and 700 °C. Vickers hardness measurements were made with a 150 g micro-indenter at room temperature (martensitic state). The latent heat of transformation was measured by a Dupont differential scanning calorimeter at a heating rate of 5 °C/min.

The increase of the latent heat as the annealing temperature increases is mainly due to the increase of the reversibility characterizing the thermoelastic austenite-martensite phase transformation. The dislocation density is reduced when a higher annealing temperature is chosen, causing a lower level of strain energy stored in the alloy. Another consequence of the reduction of the dislocation density is the decrease of hardness linked with the decrease of the material yield stress.

It was reported by Lin and Wu that stress-free thermal cycling through the transformation zone improves mechanical resistance of the material (evaluated by hardness measurement) and therefore increases the fatigue life.[4] To assess the influence of the transformation induced hardening on the evolution of the HV and latent heat (LH) characteristics, the data presented in Fig. 1 have been compared with those obtained after 20 thermal cycles performed prior to DSC and hardness testing (Fig. 2).

It was observed that the higher the annealing temperature, the lower the material hardness for both cycled and noncycled samples. However, samples annealed between 450 and 650 °C and then thermally cycled have higher hardness than the noncycled samples, while samples annealed at higher or lower temperatures do not manifest any difference in this respect (Fig. 2, center diagram). This phenomenon probably results

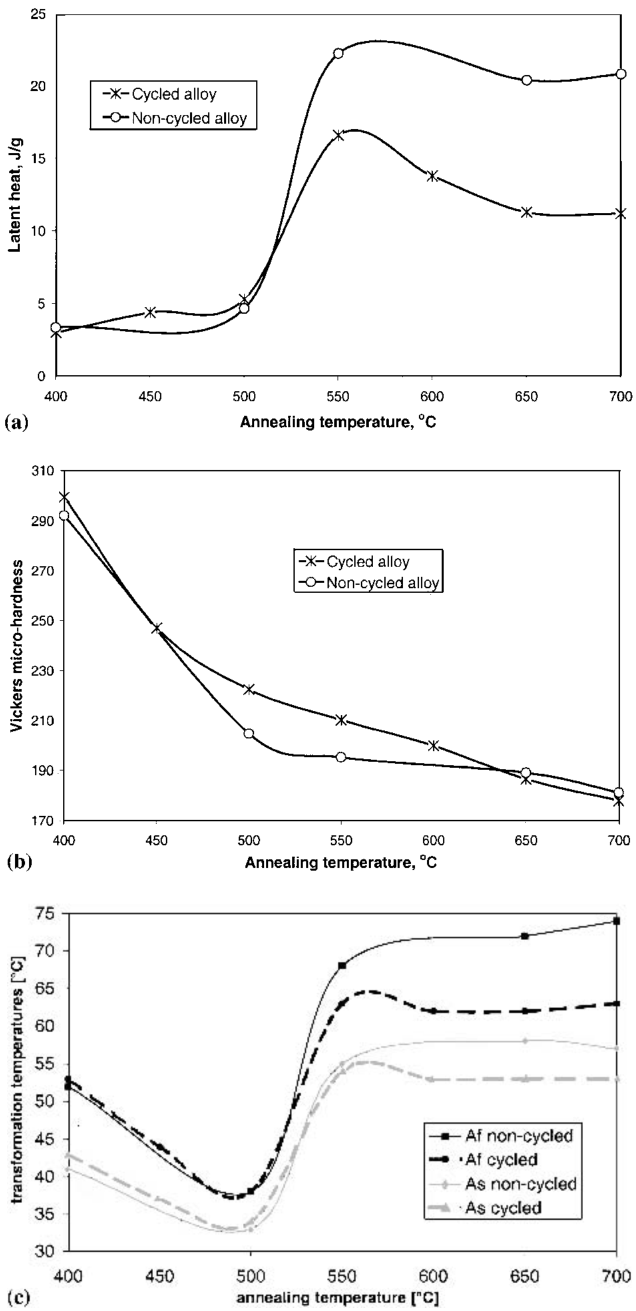

Fig. 2 Latent heat of transformation (upper diagram), microhardness of martensite (center diagram), and transformation temperatures (lower diagram) in the function of annealing temperature for cycled and noncycled NiTi samples

from the interaction between two sets of dislocations: the first set introduced during previous cold work (strain hardening), and the second one generated during thermal cycling (transformation induced hardening).

On one hand, it seems that annealing at temperatures lower than 450 °C does not affect the level of strain hardening enough to make distinguishable the effect of subsequent transformation hardening. On the other hand, annealing at temperatures higher than 600 °C results in such important softening of the material, that twenty-cycle transformation hardening is not sufficient to produce any remarkable results. Consequently, only after annealing in the 450-650 °C region, could the dislocations resulting from transformation hardening superposed on those resulting from strain hardening produce measurable effects of combined strengthening of the material.

Variations of latent heat in the function of annealing temperature (Fig. 2, top) demonstrated similar trends for cycled and noncycled samples, with maximum latent heat values at approximately 550 °C. On one hand, annealing at temperatures lower than 500 °C is not enough to ease interface movement due to severe strain hardening resulting from cold working. Therefore, thermal cycling does not produce any remarkable effect in this zone. On the other hand, the higher the annealing temperature, the more important the influence of transformation-induced hardening on the latent heat values becomes.

In Fig. 2 (lower diagram), transformation temperatures measured for cycled and noncycled samples in the function of annealing temperatures follow trends similar to the latent heat values.

It can be concluded that in the region encompassing the optimum annealing temperature (500-600 °C), the hardness of precycled samples is higher than that of those only annealed, while the latent heat is lower. Therefore, the optimization procedure could either be applied to only annealed or pre-cycled samples with similar results. In the present article, the data obtained with thermally pre-cycled (stabilized) samples are treated using Eq 4.

In Fig. 3, three curves calculated by Eq 4 are superposed on the hardness and latent heat curves normalized between 0 and 1. From this figure, it can be concluded that the best post-deformation annealing temperature for this alloy—determined under supposition of equal beneficial importance of latent heat and hardness characteristics [center curve with $w(\text{LH}) = w(\text{HV}) = 0.5$]—is about 550 °C. When the importance given to latent heat is higher than that appointed to hardness [upper curve with $w(\text{LH}) = 0.9$ and $w(\text{HV}) = 0.1$], the optimum shifts towards higher temperatures. Inversely, if the priority is given to hardness [lower curve with $w(\text{LH}) = 0.1$ and $w(\text{HV}) = 0.9$], the optimum shifts to lower temperatures.

In the following work, to assess the validity of the proposed optimization procedure, samples treated at different temperatures will be subjected to low-cycle fatigue testing. The results of this validation are presented hereafter.

5. Validation

5.1 Materials and Experimental Method

Based on the results of DSC-HV optimization, several NiTi ribbon specimens of 12 cm long, annealed for 1 h at 400, 450, 500, 550, 600, 650, and 700 °C, were thermally cycled under constant tensile stresses of 55, 130, and 180 MPa between room temperature (martensitic state) and nearly 100 °C (austenitic state). The main elements of the experimental bench are shown in Fig. 4 (upper). The load is applied by a suspended weight. Elongation of the specimen, directly heated by electrical current, is measured by a linear variable displacement transducer (LVDT) located as shown in the illustration. Temperature measurement is assured by a thermocouple placed directly

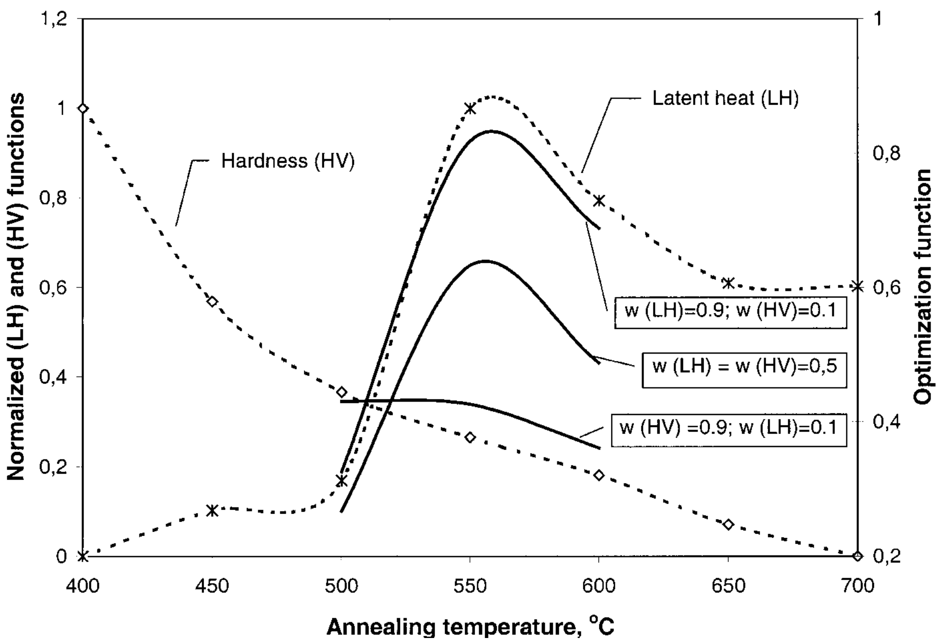

Fig. 3 Normalized latent heat of transformation (LH), hardness of the martensite (HV), and graphic representation of the optimization function in the function of annealing temperature

on the surface of the ribbon. The current source and data acquisition are controlled by a computer specifically programmed for this application. The recorded data include temperature and length variations of the specimen, as well as the number of cycles.[7]

The direct output from the thermal fatigue testing under a constant load recorded by the data acquisition system is best represented by hysteresis loops of total strain in the function of temperature as shown in Fig. 4 (lower diagram). This graph shows the evolution of the specimen behavior during thermal cycling. The values of ε_A and ε_M represent the strain of the austenite and martensite phases at each cycle. The difference $\Delta\varepsilon$ between these values corresponds to the recovery strain due to the shape memory effect. The zero strain value corresponds to the state of the specimen before applying the load.

6. Results and Discussion

The whole fatigue life of SMA can be roughly divided in three phases having different extensions depending on test conditions and material properties: phase of initial material stabilization, followed by a merely plateau behavior, and concluded by a rapid loss of dimensional and functional stability of the material. The extension of the first zone varies generally between 10 and 100 cycles, while the plateau and final phases can be encompassed between 10^2 and 10^6 cycles. Consequently, the whole procedure of experimental validation is also divided in two distinctive experiments: the first performed in the zone of initial material stabilization (10 cycles) and the second, up to 3000 thermal cycles.

6.1 Phase of Material Stabilization

During the first 10 thermal cycles, mechanical work performed by samples annealed at different temperatures is measured. To make this measure comparable with the latent heat determined by DSC testing, the first is presented as a mean specific work (work by unity of weight) calculated by the following formula:

$$W = \frac{1}{10}\left[\sum_{i=1}^{10}\frac{\sigma[\text{MPa}]\cdot A\,[\text{mm}^2]\cdot\Delta\varepsilon_i[\text{mm}]}{V\,[\text{mm}^3]\cdot\rho\,[\text{g/mm}^3]}\right] \text{ or}$$

$$W = \frac{1}{10}\left[\frac{\sigma}{\rho}\sum_{i=1}^{10}\frac{\Delta\varepsilon_i}{l}\right][\text{J/g}]$$

where σ is the constant stress; A, V, l, and ρ, the cross-section area, volume, length, and mass density of the specimen, respectively; and $\Delta\varepsilon_i$, the reversible deformation measured in each cycle.

In Fig. 5, the evolution of mean specific work generated upon heating in the function of annealing temperature and applied stress is traced. (Note that the mechanical work data are approximated here with their four-degree polynomial trendlines.) From this diagram, it can be observed that mechanical work reaches maximum values in the 475-625 °C region, which encompasses the optimum annealing temperature found after DSC-HV testing (550 °C in the case of the equal importance of latent heat and hardness). Furthermore, the higher the applied stress, the lower the temperature of the mechanical work maxima. This easily anticipated trend reflects the growing importance of the material hardening in case of increasing applied stresses. This shift of the optimum annealing temperature toward lower values corresponds to the case of increasing priority of material hardness in respect to latent heat (Fig. 3). Moreover, from Fig. 5, one can conclude that the specific mechanical work (averaged for 10 first cycles) is directly proportional to the applied stress, and therefore can be estimated in the 55-180 MPa region by the following formula:

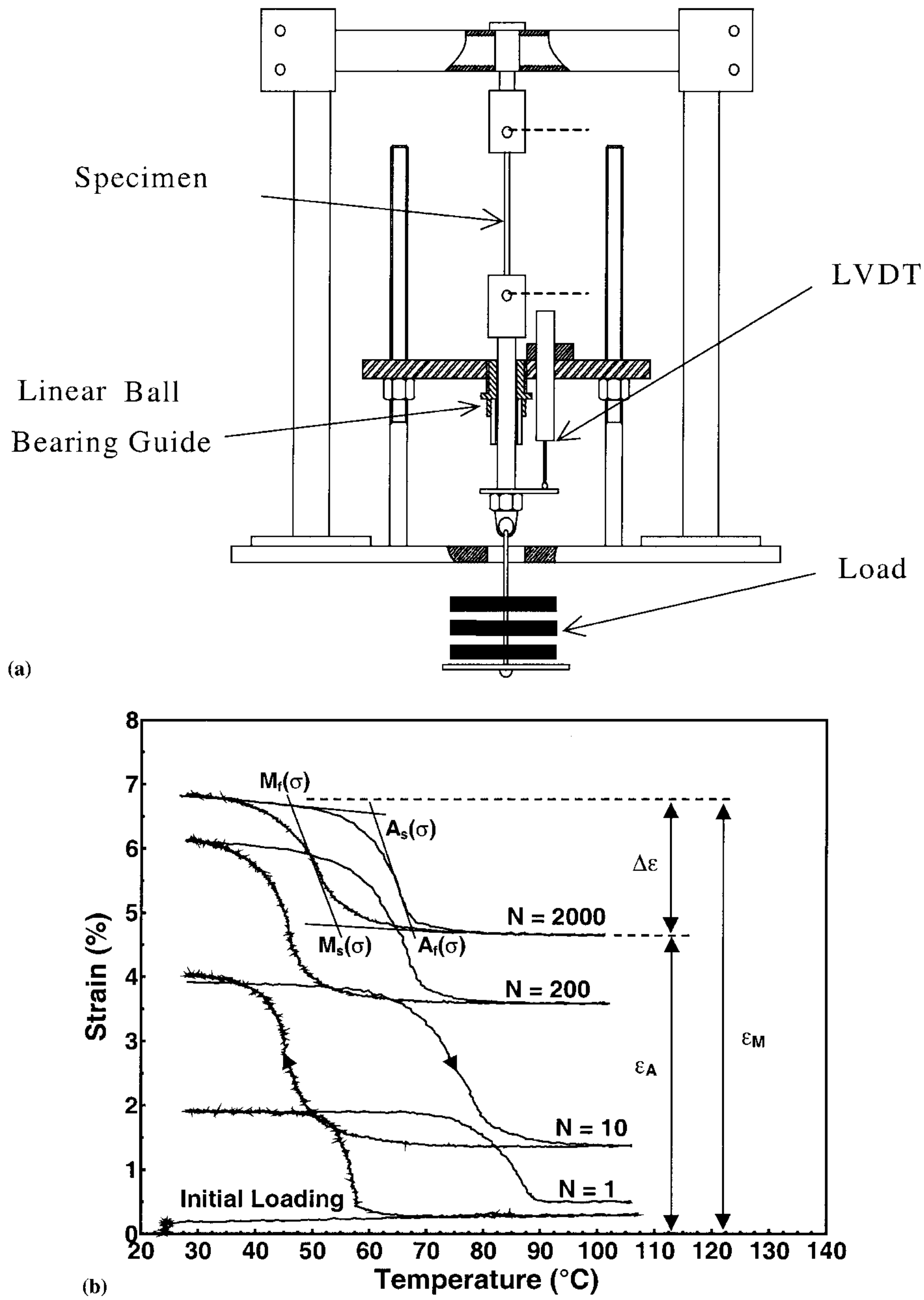

Fig. 4 Experimental bench used for thermal cycling under a constant applied load (upper drawing); definition of transformation temperatures and strains from typical hysteresis loops: ε_A, austenite strain; ε_M, martensite strain; $\Delta\varepsilon$, recoverable strain (lower diagram)

$$W\,[\mathrm{J/g}] \approx 8.13 \cdot 10^{-3} \cdot \sigma\,[\mathrm{MPa}] - 0.24$$

Finally it can be remarked that the mechanical work generated under the highest stresses applied to the specimen in this study (180 MPa) is approximately one order of magnitude lower than the specific latent heat values measured in free stress conditions by DSC (1.2 J/g versus 16 J/g).

6.2 Testing Up to 3000 Cycles

To extend our analysis in terms of the number of cycles, while focusing on the zone of interest (annealing temperatures varying between 475 and 625 °C), measurement of transformation temperatures and recoverable strain up to 3000 cycles has been performed with specimens annealed at 550 °C (temperature found on the basis of the equal beneficial importance of latent heat and hardness), 625 °C (latent heat is prioritized), and 475 °C (hardness is promoted).

The evolution of average phase transformation temperatures, $A^* = \{A_s(\sigma) + A_f(\sigma)\}/2$ and $M^* = \{M_s(\sigma) + M_f(\sigma)\}/2$ during cycling is shown in Fig. 6 for specimens annealed at 475, 550, and 625 °C and subjected to a constant stress of 55 MPa. It is clear from Fig. 6 that annealing at 475 °C does not

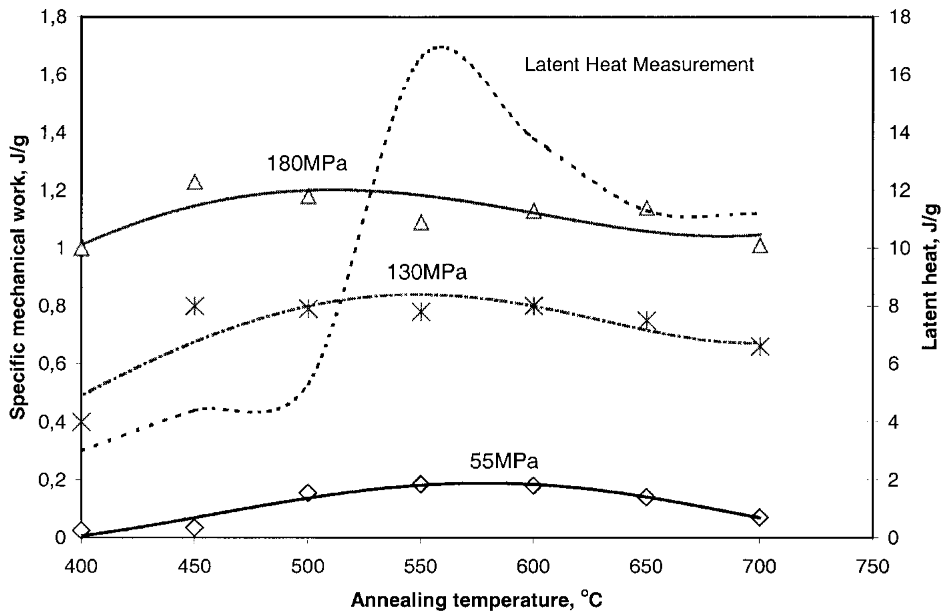

Fig. 5 Evolution of the mechanical work performed by specimens annealed at different temperatures in function of the constant stress; latent heat measured by DSC is traced for comparison

eliminate the excessively strong dislocation substructure generated by cold working, and therefore does not favor the martensite-austenite transformation. For specimens annealed at 550 and 625 °C, the increase of M^* direct transformation temperature (A → M) after nearly 50 cycles indicates an easier formation of martensite plates due to an increasing number of dislocations. These dislocations are preferentially oriented with respect to the deformation (rolling) direction and thus ease the formation of the martensite variants. The decrease of these temperatures at the beginning of the fatigue life (0-50 cycles) could be attributed to the establishment of such a dislocation structure. For the reverse transformation (M → A), the decrease of A^* temperature for specimens annealed at 550 and 625 °C reveals a beneficial effect of the same dislocation substructure that serves as a network of nucleation sites for the austenite phase and therefore facilitates the M → A transformation. Based on the obtained results, however, neither annealing at 475 and 625 °C or at 550 °C can be preferred from the point of view of the stability of transformation temperatures during thermal cycling.

During cycling up to about 10-15 cycles for all annealing temperatures, the more important increase of the martensite strain compared to the austenite strain results in a net increase of the recoverable strain $\Delta\varepsilon$ (Fig. 7). After 15 cycles, different trends are observed for these three cases of annealing. After annealing at 475 °C, the overall fatigue behavior remains unstable up to 200 cycles and then stabilizes at a recovery strain level of 2.2% up to at least 3000 cycles. Annealing at 550 °C does not eliminate completely irreversible changes during cycling, but guarantees stable behavior up to 1000 cycles at 2.75% recovery strain level. After annealing at 625 °C, the highest—comparatively to two previous cases—recovery strains are observed during the very first cycles. In this case, however, recovery strain reaches its peak at the 50th cycle and then continuously decreases.

It should be recalled, however, that the optimum annealing temperature corresponding to 550 °C has been determined on the basis of the equal beneficial importance of the two main measurable parameters: latent heat and material hardness. With respect to the fatigue behavior of the alloy, the relative value of the first parameter reflects the amplitude of the memory effect, while the relative value of the second reflects the possibility to keep this effect stable during cycling.

Let us consider for example, that the stability of the memory effect is of higher importance than its amplitude. In this case, the optimum annealing temperature obtained with the help of Eq 4 shifts to lower temperatures. As a result, at 475 °C (Fig. 7), the extension of the strain plateau is higher than that at 550 °C (2500 cycles versus 1000 cycles), and this gain is reached at the expense of the maximum recovery strain (2.2% for the 475 °C curve versus 2.75% for the 550 °C curve). On the other hand, samples annealed at 625 °C show the highest recovery strains during the very first cycles, but this gain is reached at the expense of the shape memory effect stability.

Therefore, by manipulating the relative importance weights for the material hardness or latent heat, one could use the present optimization procedure to promote either amplitude or stability of the memory effect depending on the needs of a specific application. Finally, one can conclude that annealing at 550 °C should be considered here as the most preferable annealing temperature from the overall behavior point of view (including the level and the stability of the output) determined on the basis of 3000 cycle testing under 55 MPa applied constant stress.

7. Conclusion

Thermomechanical treatment can be beneficially used to improve the fatigue life. This procedure increases the materi-

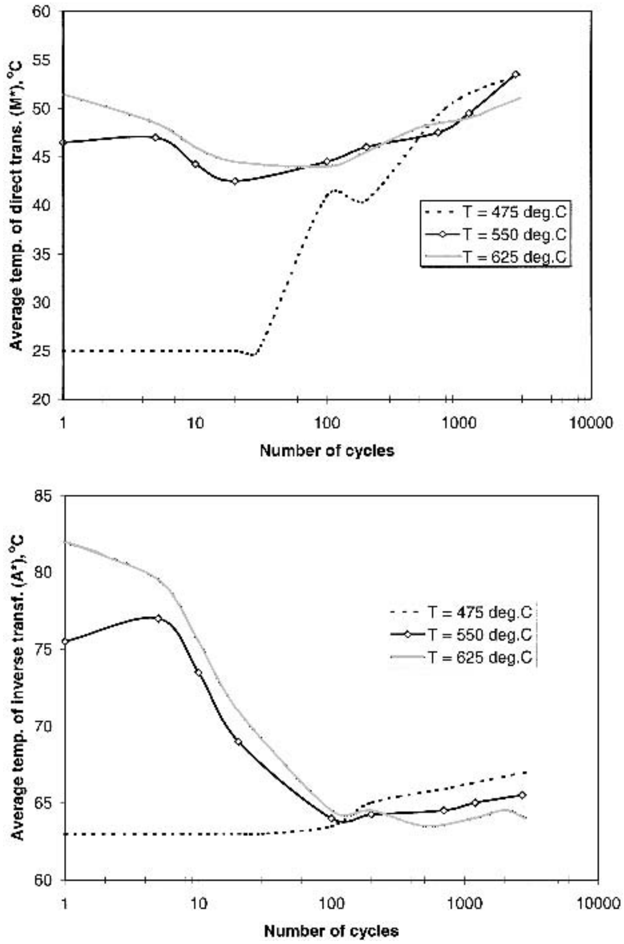

Fig. 6 Evolution of direct (upper diagram) and reverse (lower diagram) transformation temperatures during thermal cycling under a constant stress of 55 MPa after annealing at different temperatures

al's slip level, thus preventing permanent deformation during cycling and ensuring dimensional and functional stability of SMA devices. The optimum cold-work and annealing conditions should be experimentally determined for each material.

In this article, it is suggested to combine two widely used techniques: DSC and hardness testing to optimize post-deformation annealing heat treatment for Ni-50.1%Ti shape memory alloys.

The SAW, one of the numerous techniques of MCDM, is used to find a best trade-off in latent heat of transformation, measured by DSC, and material strengthening, assessed by Vickers microhardness testing.

The optimum annealing temperature, determined under supposition of equal beneficial importance of these two parameters, allowed a marked improvement of the overall fatigue behavior of nearly equiatomic NiTi samples.

It should be pointed out, however, that the reasonable establishment of the relative importance weights for material characteristics remains the most delicate procedure, which should be performed by the application engineer with respect to functional requirements of each particular application.

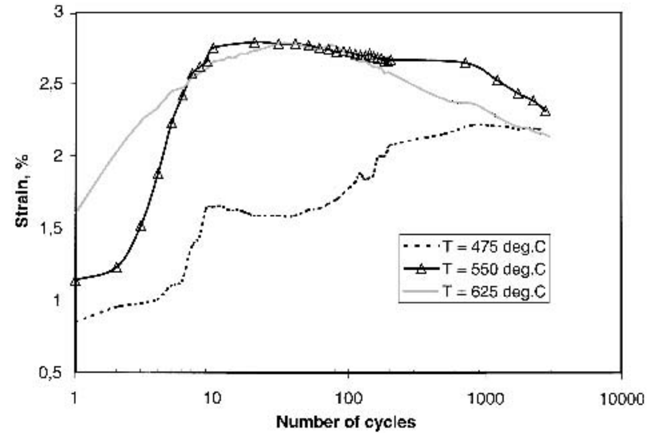

Fig. 7 Evolution of recoverable strain $\Delta\varepsilon$ during thermal cycling under a constant stress of 55 MPa after annealing at different temperatures

Acknowledgments

This work was been performed in the framework of the research program supported by the Natural Sciences and Engineering Research Council of Canada (NSERC). The authors would like also to express their sincere gratitude to Dr. S. Turenne and Dr. F. Trochu for useful discussions as well as to Mr. N. Sacépé and Mr. B. Lauenberger for their help in performing this study.

References

1. S. Miyazaki: "Thermal and Stress Cycling Effects and Fatigue Properties of Ni-Ti Alloys" in *Engineering Aspects of Shape Memory Alloys,* T. Duerig, ed., Butterworth-Heinemann, London, UK, 1990, pp. 374-403.
2. J. Marquez, T. Slater, and F. Sczerzenie: "Determining the Transformation Temperatures of NiTi Alloys Using Differential Scanning Calorimetry" in *Proceedings. Second International Conference on Shape Memory and Superelastic Technologies (SMST-97)*, Pacific Grove, CA, 1997, pp. 13-18.
3. Y. Xu, S. Shimizu, Y. Suzuki, K. Otsuka, T. Ueki, and K. Mitose, "Recovery and Recrystallization Processes in Ti-Pd-Ni High-Temperature Shape Memory Alloys," *Acta Mater.,* 1997, *45*(4), pp. 1503-11.
4. H.C. Lin and S.K. Wu: "The Tensile Behavior of a Cold-Rolled and Reverse-Transformed Equiatomic TiNi Alloy," *Acta Metall. Mater.,* 1994, *42*(5), pp. 1623-30.
5. E. Hornbogen and E. Kobus: "Characterization of Shape Memory Alloys by Hardness Indentations," *Prakt. Metallogr,* 1993, *30*(10), pp. 507-19.
6. C.L. Hwang and K. Yoon: *Multiple Attribute Decision Making, Methods and Applications*, Springer Verlag, Berlin, NY, 1981, p. 259.
7. S. Turenne, S. Prokoshkin, V. Brailovski, and N. Sacépé: "Combined Analysis of the Assisted Two-way Shape Memory Effect in NiTi," *Canadian Metall. Quarterly,* 2000, *39*(2), pp. 217-24.
8. J. Van Humbeeck: "Cycling Effects, Fatigue and Degradation of Shape Memory Alloys," *J. de Physique IV, Colloque C4,* 1991, *1,* pp. 189-97.
9. E. Hornbogen: "Fatigue of Copper-Based Shape Memory Alloys" in *Engineering Aspects of Shape Memory Alloys,* T. Duerig, ed., Butterworth-Heinemann, London, UK, 1990, pp. 267-80.